

Correlated adatom trimer on metal surface: A continuous time quantum Monte Carlo study

V. V. Savkin,^{1,*} A. N. Rubtsov,² M. I. Katsnelson,¹ and A. I. Lichtenstein³

¹*Institute of Molecules and Materials, University of Nijmegen, 6525 ED Nijmegen, The Netherlands*

²*Department of Physics, Moscow State University, 119992 Moscow, Russia*

³*Institute of Theoretical Physics, University of Hamburg, 20355 Hamburg, Germany*

The problem of three interacting Kondo impurities is solved within a numerically exact continuous time quantum Monte Carlo scheme. A suppression of the Kondo resonance by interatomic exchange interactions for different cluster geometries is investigated. It is shown that a drastic difference between the Heisenberg and Ising cases appears for antiferromagnetically coupled adatoms. The effects of magnetic frustrations in the adatom trimer are investigated, and possible connections with available experimental data are discussed.

PACS numbers: 71.10.-w, 71.27.+a, 73.22.-f

The electronic structure of adatoms and clusters on surfaces constitutes one of the most fascinating subjects in condensed matter physics and modern nanotechnology [1]. The scanning tunneling microscopy (STM) or spectroscopy technique allows the study of atomic structure, the electronic energy spectrum, and magnetic properties of different surfaces at an atomic scale. In particular, STM gives the unique opportunity of directly investigating an essentially many-body phenomenon, namely the Kondo effect [2, 3, 4]. Earlier only indirect methods such as analysis of temperature and magnetic field dependencies of thermodynamic and transport properties were available [5, 6]. Recently STM studies of small transition metal nanoclusters on different surfaces have been performed, including Co dimers [7] and Cr trimers [8] on a Au surface, and Co clusters on carbon nanotubes [9]. The electron spectrum of these nanosystems, in particular the existence of the Kondo resonance, turns out to be very sensitive to the geometry of the clusters as well as to the type of magnetic adatoms. The later can be important for nanotechnological fine tuning of surface electronic structure.

The “quantum-corrall” type of STM-experiments provides an unique opportunity to investigate in detail an interplay between the single-impurity Kondo effect and interatomic magnetic interactions in nanoclusters which is a key phenomenon in Kondo lattice physics [10, 11, 12, 13, 14]. The interaction between itinerant electrons and localized ones leads to the screening of the magnetic impurity moment which is the Kondo effect; on the other hand, the RKKY exchange interaction between localized spins suppresses the Kondo resonance at the Fermi level. As a result, a very complicated phase diagram can be obtained with regions described by a strong coupling regime, “normal” magnetic behavior with logarithmic corrections, and non-Fermi-liquid behavior [11]. Quantum critical points at the boundary of different phases is a subject of special interest [12, 14]. There exists a general belief that anomalous features of many f -electron systems such as heavy-fermion or non-Fermi-

liquid behavior can be treated in terms of the Kondo lattice picture [6, 15, 16]. This is why non-perturbative investigations of the basic physical features of few-atom magnetic clusters in a metallic medium is of primary interest. At the same time, due to the extreme complexity of the problem, theoretical investigations of electronic structure for several Kondo centers usually involve some uncontrollable approximations, such as a replacement of the Heisenberg interatomic exchange interactions by the Ising ones [14] or a variational approach based on a simple trial function [17].

In this Letter we present results of a numerically exact solution of the three Kondo impurity problem within the recently developed continuous time quantum Monte Carlo (CT-QMC) method [18]. For the antiferromagnetic (AFM) exchange interatomic interaction, in contrast to the ferromagnetic (FM) one, the results for the Heisenberg and Ising systems differ essentially. Based on our theoretical analysis, the recent paradoxical experimental results [8] where the Kondo resonance is observable for an isosceles magnetic triangle but not for the perfect Cr-trimer or individual Cr adatom will be discussed.

We start with the system of three impurity correlated sites with Hubbard repulsion U in a metallic bath and with an effective exchange interaction J_{ij} between them, a minimal model which however includes all relevant interactions necessary to describe magnetic nanoclusters on a metallic surface. The effective action for such cluster in a metallic medium has the following form:

$$S = S_0 + W, \quad (1)$$

$$S_0 = - \int_0^\beta \int_0^\beta d\tau d\tau' \sum_{i,j;\sigma} c_{i\sigma}^\dagger(\tau) \mathcal{G}_{ij}^{-1}(\tau - \tau') c_{j\sigma}(\tau'),$$

$$W = \int_0^\beta d\tau \left(U \sum_i n_{i\uparrow}(\tau) n_{i\downarrow}(\tau) + \sum_{i,j} J_{ij} \mathbf{S}_i(\tau) \mathbf{S}_j(\tau) \right).$$

The last term in the right-hand-side of Eq.(1) allows us to consider the most important “Kondo lattice” feature, that is, the mutual suppression of the Kondo screening and intersite exchange interactions [10, 11]. Another factor, the coherence of the resonant Kondo scattering, is

taken into account by the introduction of inter-impurity hopping terms t_{ij} to the bath Green function which is supposed to be $\mathcal{G}_{ij}^{-1} = \mathcal{G}_i^{-1}\delta_{ij} - t_{ij}$. Here $\mathcal{G}_i^{-1}(i\omega_n) = \mu + i(\omega_n + \sqrt{\omega_n^2 + 1})/2$ corresponds to the semicircular density of states (DOS) with band-width 2 and t_{ij} are inter-impurity hopping integrals. For real adatom clusters the exchange interactions are mediated by conduction electrons (RKKY interactions) which are dependent on the specific electronic structure of both adatoms and host metal. To simulate this effect we will consider J_{ij} as independent parameters which is a common practice in the Kondo lattice problem [10, 11, 14]; otherwise for the half-filled non-degenerate Hubbard model used in our calculations the exchange is always antiferromagnetic. In the model (1) the geometry of the problem is specified by the values of exchange integrals J_{ij} and hopping parameters t_{ij} [19]. We will concentrate on the case of equilateral triangle when $J_{ij} = J$ and $t_{ij} = t$; to compare with the experimental situation in Ref.8 also an isosceles triangle will be considered. To check an approximation used in Ref.14 we will investigate the case when all spin-flip exchange terms are ignored and the Heisenberg (**SS**) form of interaction $J_{ij}\mathbf{S}_i(\tau)\mathbf{S}_j(\tau)$ is transformed into the Ising (S_zS_z) one $J_{ij}S_i^z(\tau)S_j^z(\tau)$.

We use the numerically exact CT-QMC method [18] for our computer simulations. Unlike the Hirsh-Fye discrete-time scheme [20] it does not involve auxiliary Ising spins, but performs a random walk in the space of terms of the perturbation expansion for the Green function. One of the advantages of this novel approach is the opportunity it provides to study systems with non-local (in space and in time) interactions, which in the usual Hirsh-Fye approach would involve a huge increase in the required number of auxiliary fields and time slices [18].

In brief, numerical simulations make use of the division of the action into Gaussian and interaction parts. The later can be presented in the form $\int d\tau \sum w_{ijij'}(\tau)$, where $w = u_{ijij'}(c_{i,\uparrow}^\dagger c_{j,\uparrow} - \alpha_\uparrow)(c_{i',\downarrow}^\dagger c_{j',\downarrow} - \alpha_\downarrow)$, where the α 's are c -numbers chosen in a special way to minimize the sign problem in the QMC simulation. It is worth noting that only the presence of these α 's makes possible the simulation of systems with repulsive forces [18].

The formal interaction-representation expansion in powers of the interaction for the Green function $G_{ij}(\tau, \tau')$ reads

$$\sum_k \sum_{I_1, \dots, I_k} \int d\tau_1 \dots d\tau_k \frac{\text{Tr} \left(T c_{i\tau}^\dagger c_{j\tau} w_{I_1}(\tau_1) \dots w_{I_k}(\tau_k) \right)}{Zk!}. \quad (2)$$

Here Z is the partition function and I denotes the set i, j, i', j' . Our algorithm performs the random-walk in a space of all possible values for $k; \tau_1 \dots \tau_k; I_1 \dots I_k$. The numerical averaging of Eq.(2) over this random walk gives the desired Green function for the interacting system with the action (1). Typical value for k in our calcu-

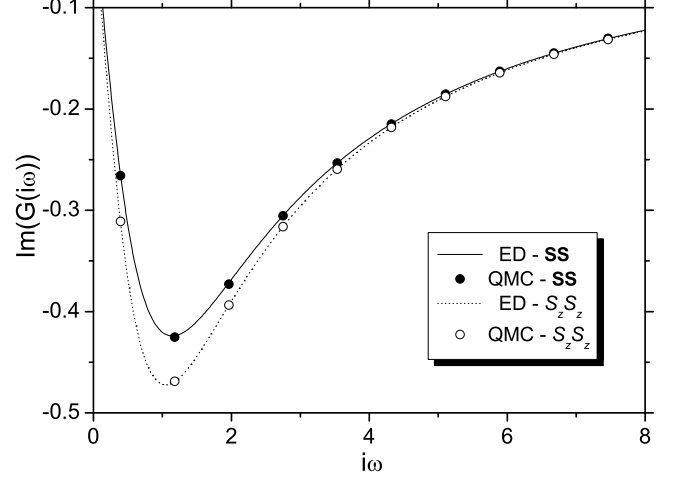


FIG. 1: Imaginary part of the Green function at Matsubara frequencies for the model (1) with $\mathcal{G}_i^{-1}(i\omega_n) = \mu + i\omega_n$ for **SS** and S_zS_z interactions. Symbols are CT-QMC data, lines are exact diagonalization (ED) results. Parameters of the model: $U = 2, J = 0.2, t = 0, \beta = 8, \mu = U/2$.

lation is $k \approx \int d\tau \sum ||w_I(\tau)|| \approx N\beta U + N^2\beta J$, where β is the inverse temperature and N is number of atoms in the cluster. One can see that for the case $U \gg NJ$ the exchange interaction indeed does not slow the calculation down, its complexity is determined by the local (Coulomb) interaction.

In order to check the CT-QMC algorithm for a system with complicated Heisenberg interactions we apply this method to a simple Hamiltonian analogue of the model (1), *i.e.* for $\mathcal{G}_i^{-1}(i\omega_n) = \mu + i\omega_n$. We compare our CT-QMC approach with the solution obtained using the exact diagonalization method. Results for the system with AFM J ($J > 0$) are shown in Fig.1 for S_zS_z and **SS** interactions. The estimated errorbar in numerical data is 10^{-3} or less.

Although the problem of DOS-calculations from $G(\tau)$ data is ill-defined, quite reliable estimations can be made at our level of the numerical accuracy. For example, DOS of the above-mentioned Hamiltonian models is at most contributed by the four δ -peaks located at $\pm U/2, \pm(U/2 + J)$ for Ising and $\pm U/2, \pm(U/2 + 2J)$ for Heisenberg interaction. Fit of the numerical data with several δ -peaks indeed resolves their positions (with a 5% errorbar) and relative heights (with a 20% errorbar). Further, we study models with a continuous DOS, and standard maximum-entropy analytical continuation method [21] is used to recover DOS. Normally it resolves the DOS features from imaginary time QMC data with a similar accuracy.

Let us discuss correlated adatom trimer in the metallic bath depending on type of the effective exchange interaction (S_zS_z or **SS**) for AFM and FM cases. First we show that **SS** type of interaction suppresses the reso-

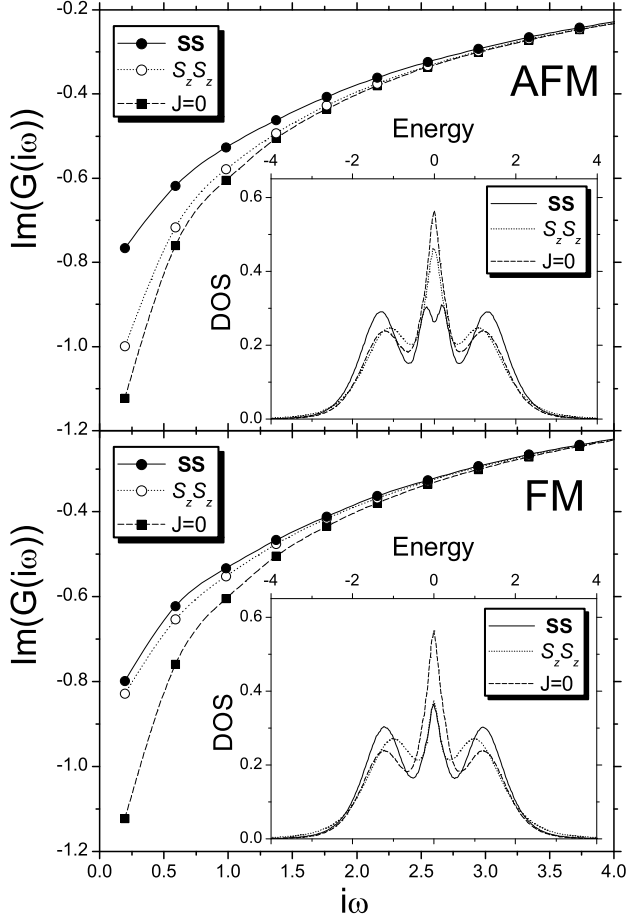


FIG. 2: Imaginary part of the Green functions at Matsubara frequencies for the correlated adatom equilateral triangle in the metallic bath for AFM (upper figure) and FM (lower figure) types of effective exchange interaction. Parameters: $U = 2, J = \pm 0.2, t = 0, \beta = 16, \mu = U/2$. There are three dependencies on each picture for **SS**, $S_z S_z$ and $J = 0$ (which corresponds to single atom in the metallic bath) types of interaction. The insets show DOS.

nance in AFM case. We study the equilateral triangle at half-filling. The Green functions at the Matsubara frequencies obtained by the CT-QMC technique and corresponding DOS are presented in Fig. 2. The case of $J = 0$ corresponds to the single Kondo impurity in the bath. One can see that there is no essential difference between $S_z S_z$ and **SS** types of interaction in FM but for the AFM one this difference is very important. The AFM **SS** interaction leads to pronounced suppression of the Kondo resonance at Fermi level for physically relevant values of J (Fig. 2). On the other hand, in the FM case we do not observe any essential difference between the $S_z S_z$ and **SS** types of the interaction for a wide range of the model parameters.

To explain these results we need to calculate the spectral density $D(\omega)$ of the on-site spin-flip operators S_i^\pm for

an AFM equilateral triangle $D_{\text{SS}}(\omega) = \frac{2}{3}\delta(\omega) + \frac{1}{3}\delta(\omega - 3J)$, $D_{S_z S_z}(\omega) = \frac{1}{3}\delta(\omega) + \frac{2}{3}\delta(\omega - 2J)$. In both cases there is a part of the spectral density with zero frequency due to degeneracy of the ground state and spin-flip transitions between its components, but for the **SS** case this part is twice as large. For the case $J \gg T_K$ (T_K is one-site Kondo temperature) only this “soft” component of the spectral density will lead to Kondo screening which means that the suppression of the Kondo effect is twice more efficient for the **SS** case than for the $S_z S_z$ one. Since the trimer as a whole has a degenerate ground state there is still a strong-coupling regime and an effective Kondo temperature T_K^* which however is much smaller than T_K . Scaling considerations similar to one proposed in Ref.11 gives an estimation of $T_K^* \simeq T_K^{3/2}/J^{1/2}$ and $T_K^* \simeq T_K^3/J^2$ for the **SS** and $S_z S_z$ case respectively. We assume that this quantity is too small to be visible in our simulations (as well as in the experimental data [8]) so what is observed corresponds to the one-site Kondo resonance at the condition $T_K \geq J$. Similar estimation for the case of FM interactions shows that there is no difference between the $S_z S_z$ and **SS** model there and $T_K^* \simeq T_K^3/J^2$ as in the AFM $S_z S_z$ case.

In order to describe the experimental situation we changed the geometry of the adatom trimer. An observation of the Kondo resonance reconstruction was reported for one isosceles geometry of three Cr atoms on a gold surface [8]. Thus we study the isosceles triangles for AFM and FM types of effective exchange interaction. We have chosen the following parameters of J_{ij} to imitate the experimental system: $J_{23} = J, J_{12} = J/3, J_{13} = J/3$. The computational results are presented in Fig. 3, where one can see the reconstruction of resonance in AFM and FM cases in accordance with experimental data. Note that the Kondo resonance appears only for the more weakly bonded adatom in AFM case.

The observed picture can be drastically changed by introducing a non-zero value of the hopping parameter t_{ij} . As noted above the trimer ground state is degenerate at $t_{ij} = 0$, however this degeneracy is lifted for $t_{ij} \neq 0$. If one of the obtained states lies below the Fermi level, DOS can be changed drastically and at certain parameters it leads to the appearance of a resonance on the Fermi level (see Fig.4). In Fig.4, DOS is shown for various values of filling in the system and at nonzero t_{ij} . It is necessary to point out that the introduction of the parameter t_{ij} , the variation of the filling in the system (μ), and different geometries (J_{ij}) can lead to various results in DOS. This can be used as one of the possible explanations of the experimental data regarding the Cr trimer on a Au surface which look initially appear counter-intuitive: the Kondo temperature for the trimer is much larger than for the single site, despite the suppression of the Kondo effect by J_{ij} . One can assume that this is a consequence of the change of the number of d -electrons in ground-state configuration for the Cr atom in the trimer in comparison

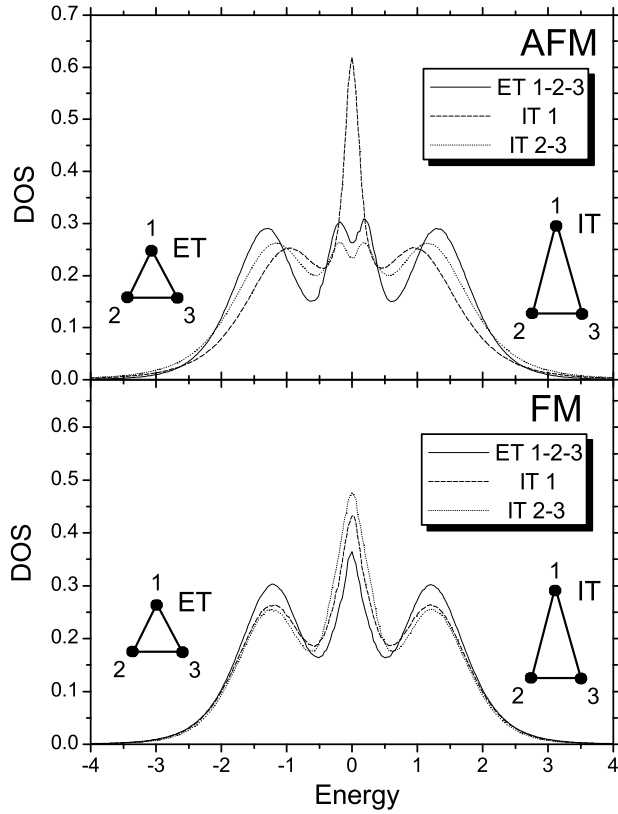


FIG. 3: DOS for equilateral triangle (ET) and isosceles triangle (IT) geometries with AFM (upper figure) and FM (lower figure) types of effective exchange interaction. Parameters are the same as in Fig.2. Values of the effective exchange integrals for IT are as follows: $J_{23} = J$, $J_{12} = J/3$, $J_{13} = J/3$. There are two dependencies in case of IT: one for adatom 1 and another for equivalent adatoms 2 and 3. All adatoms are equivalent in the case of ET (one dependence).

with the isolated one. In order to describe specific experimental results quantitatively the method developed here should be combined with first-principle calculations in the spirit of recently developed “local density approximation plus dynamical mean-field theory” (LDA + DMFT) scheme [22].

In conclusion, we have shown that the electronic structure of a correlated adatom trimer on a metallic surface drastically depends on the symmetry of magnetic interactions. The effective exchange interaction of \mathbf{SS} type leads to more efficient suppression of the Kondo resonance in the AFM case than in the case of $S_z S_z$ interactions. The experimental STM data [8] can be reproduced qualitatively well by variation of the geometry of the problem, hopping integrals and electronic filling for magnetic nanosystems.

The work was supported by FOM project N0703M, NWO project 047.016.005 and “Dynasty” foundation.

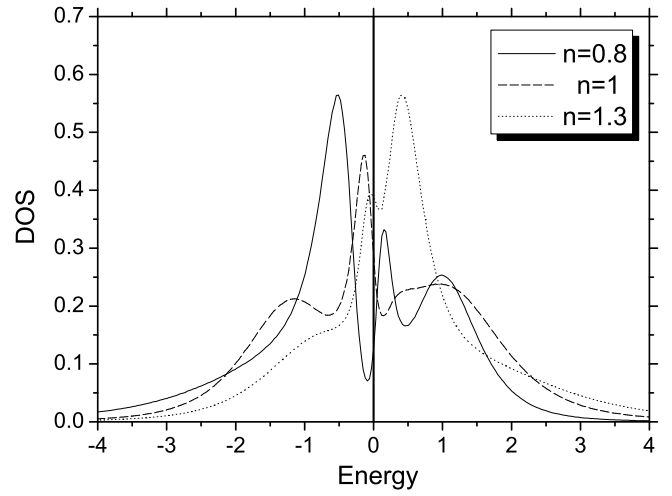


FIG. 4: DOS for equilateral triangle with an AFM type of effective exchange interaction at various values of filling in the system. Parameters: $U = 2$, $J = 0.2$, $t = 0.3$, $\beta = 16$. Corresponding numbers of particles are $n = 0.8$, $n = 1$ (half-filled case) and $n = 1.3$.

* Electronic address: savkin@sci.kun.nl

- [1] For review, see special issue of *Surf. Sci.* **500**, 1-1053 (2002), ed. by C. B. Duke and E. W. Plummer; especially E. W. Plummer et al, *Surf. Sci.* **500**, 1 (2002); J. Schen and J. Kirschner, *Surf. Sci.* **500**, 300 (2002).
- [2] V. Madhavan et al, *Science* **280**, 567 (1998); J. Li et al, *Phys. Rev. Lett.* **80**, 2893 (1998).
- [3] H. C. Manoharan et al, *Nature* **403**, 512 (2000).
- [4] O. Yu. Kolesnichenko et al, *Nature* **415**, 507 (2002).
- [5] G. Grüner and A. Zawadowski, *Rep. Prog. Phys.* **37**, 1497 (1974).
- [6] A. C. Hewson, *The Kondo Problem to Heavy Fermions*, Cambridge University Press, Cambridge, 1993.
- [7] W. Chen et al, *Phys. Rev. B* **60**, R8529 (1999).
- [8] T. Jamneala et al, *Phys. Rev. Lett.* **87**, 256804 (2001).
- [9] T. W. Odom et al, *Science* **290**, 1549 (2000).
- [10] S. Doniach, *Physica B* **91**, 231 (1977).
- [11] V. Yu. Irkhin and M. I. Katsnelson, *Phys. Rev. B* **56**, 8109 (1997); *ibid.* **59**, 9348 (1999); *ibid.* **61**, 14640 (2000).
- [12] Q. Si et al, *Nature* **413**, 804 (2001).
- [13] E. Novais et al, *Phys. Rev. B* **66**, 174409 (2002).
- [14] J.-X. Zhu et al, *Phys. Rev. Lett.* **91**, 156404 (2003).
- [15] G.R. Stewart, *Rev. Mod. Phys.* **56**, 755 (1984); *ibid.* **73**, 797 (2001).
- [16] A. Amato, *Rev. Mod. Phys.* **69**, 1119 (1997).
- [17] Yu.B. Kudasov and V.M. Uzdin, *Phys. Rev. Lett.* **89**, 276802 (2002).
- [18] A. N. Rubtsov and A. I. Lichtenstein, *JETP Lett.* **80**, 61 (2004); A. N. Rubtsov, cond-mat/0302228.
- [19] A. Georges et al, *Rev. Mod. Phys.* **68**, 13 (1996).
- [20] J. E. Hirsch and R. M. Fye, *Phys. Rev. Lett.* **56**, 2521 (1986).
- [21] M. Jarrell and J. E. Gubernatis, *Phys. Rep.* **269**, 133 (1996).
- [22] V. I. Anisimov *et al.*, *J. Phys.: Condens. Matter* **9**, 7359

(1997); A. I. Lichtenstein and M. I. Katsnelson, Phys. Rev. B **57**, 6884 (1998).